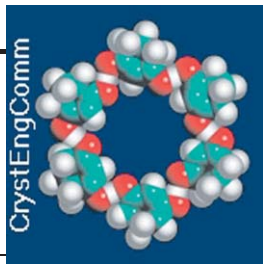

Supramolecular porphyrin-based materials. Assembly modes of [5,10,15,20-tetrakis(4-hydroxyphenyl)porphyrinato]zinc with bipyridyl ligands†

Paper

Yael Diskin-Posner, Goutam Kumar Patra and Israel Goldberg*

School of Chemistry, Sackler Faculty of Exact Sciences, Tel Aviv University, 69978 Ramat Aviv, Tel Aviv, Israel. E-mail: goldberg@post.tau.ac.il

Received 29th April 2002, Accepted 17th May 2002
Published on the Web 16th July 2002

Reaction of [5,10,15,20-tetrakis(4-hydroxyphenyl)porphyrinato]zinc with bipyridyl-type ligands leads to the formation of extended three-dimensional supramolecular architectures sustained by a concerted mechanism of metal–ligand (pyridyl-N···Zn) coordination and cooperative intermolecular (O–H···OH and O–H···N) hydrogen bonding. The competing nature of these interactions, along with the different length and functionality of the ligand auxiliaries, affects the resulting motifs of the porphyrin–ligand supramolecular assembly. Herein we describe new heterogeneous complexes of this type, and evaluate the various modes of intermolecular association in these materials.

Introduction

Targeted synthesis of stable network materials, by design, presents an exciting challenge in molecular chemistry.[1,2] It requires suitably instructed building blocks that are programmed by virtue of their structure and functionality to spontaneously self-assemble into multi-dimensional polymeric arrays.[3] The important role played by metalloporphyrins in mediating electron and energy transfer, their utility as redox catalysts, and their dynamic photophysical properties,[4] have stimulated extensive interest in the supramolecular chemistry of these systems. Recently, a series of new porphyrin-based molecular-sieve-type materials, some with pores of nano-sized dimensions, have been successfully synthesized, wherein directed metal–ligand coordination as well as cooperative hydrogen bonding play an extremely effective role in the formulation of such extended supramolecular architectures.[5,6] The different crystal-engineering strategies applied by us to this end have been reviewed recently, building on the molecular recognition functionality of the tetracarboxy and tetrapyridyl metalloporphyrin derivatives.[7] In a similar context we have introduced earlier the [5,10,15,20-tetrakis(4-hydroxyphenyl)-porphyrinato]zinc moiety (**1**) as a potentially useful tecton unit for the construction of multiporphyrin arrays, and characterized its basic self-complementary hydrogen bonding features.[8] It was shown that the supramolecular assembly of **1** is most commonly characterized by direct hydrogen bonding interactions between the *cis*-related arms of adjacent species parallel to the porphyrin planes, yielding either one-dimensional chains or flat two-dimensional patterns. These motifs contain open spaces between the interconnecting porphyrin units, of approximate van der Waals dimensions of 4 × 9 Å, that are accessible to guest molecular components. The axial coordination features of metalloporphyrins with imino and amine ligands have been extensively studied as well.[9] In this paper we discuss our successful efforts with porphyrin **1** (Scheme 1) to combine the two molecular recognition algorithms within the same material with the aid of bipyridyl-type ligand auxiliaries (**2**–**4**; Scheme 1). Initial findings of the unique supramolecular motifs formed by interaction of **1** with the shorter ligands **3** and **4** have been reported very recently in a preliminary communication.[10] The interaction mode of **1** with the longer ligand **2** is described below, along with a comparative discussion of the observed 3-D architectures in the three compounds. The reported results illustrate realization of supramolecular assembly of porphyrin-based materials *via* new synthons of extended non-covalent connectivity in three-dimensions.

Experimental

The analyzed compound **5** was obtained by reacting equimolar (0.01 mmol) amounts of the porphyrin (**1**) and the organic ligand (**2**) components in 4 ml of hot methanol. To the resulting solution was added 0.25 ml of nitrobenzene as template.[11] Single crystals of the heterogeneous supramolecular assembly were obtained by slow evaporation as a nitrobenzene and water solvate. The X-ray measurements (Nonius KappaCCD diffractometer) were carried out at *ca.* 110 K, on a crystal coated with a thin layer of amorphous hydrocarbon oil in order to minimize deterioration, possible structural disorder and related thermal motion effects, and to optimize the precision of the crystallographic results. The crystal structure was determined with DIRDIF-96 and refined with SHELXL-97 computer programs.[12,13] Hydrogen atoms attached to carbon were

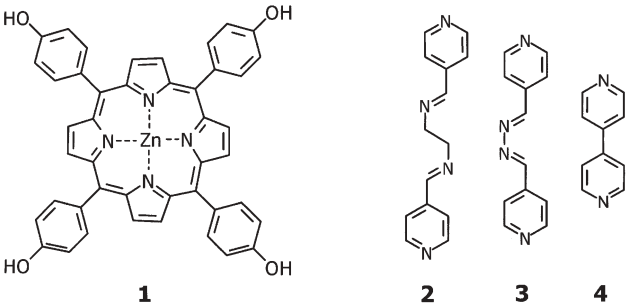

Scheme 1 Porphyrin buiding block (**1**) and the bipyridyl ligand auxiliaries (**2**–**4**) used in this study. The different porphyrin–ligand assemblies **5**, **6** and **7** discussed below relate to the **1** : **2**, $(\mathbf{1})_2$: $(\mathbf{3})_3$, and $(\mathbf{1})_2$: **4** supramolecular complexes, respectively.

†Based on the presentation given at CrystEngComm Discussion, 29th June–1st July 2002, Bristol, UK.

 DOI: 10.1039/b204129b

Table 1 Crystallographic data for **5**[a]

Parameter	**5**
Formula[b]	$[(C_{44}H_{28}N_4O_4Zn)\cdot(C_{14}H_{14}N_4)\cdot 4(C_6H_5NO_2)\cdot(H_2O)]$
M	1490.82
Crystal system	Monoclinic
Space group	$P2_1/c$
a/Å	14.6200(2)
b/Å	30.6550(4)
c/Å	16.5280(3)
β/°	103.947(1)
V/Å^3	7189.1(2)
Z	4
T/K	110
D_c/g cm^{-3}	1.377
μ(MoKα)/mm^{-1}	0.42
$2\theta_{max}$/°	51.6
Unique reflections	13 640
Refined parameters	1042
Final R_1, observations [$I > 2\sigma(I)$]	0.066, 8898
R_1 (all unique data)	0.116
wR_2 (all unique data)	0.189
Final $\lvert\Delta\rho\rvert$[c]/e Å^{-3}	$\leqslant$0.60

[a]Click here for full crystallographic data (CCDC 184848). [b]Three of the nitrobenzene molecules are located at general positions and exhibit partial disorder. Two other nitrobenzenes are located on, and disordered about, centers of inversion. [c]Except for two residual peaks (1.28 and 0.96 e Å^{-3}) near one of the disordered nitrobenzene species (which could not be well modeled).

located in calculated positions to correspond to standard bond lengths and angles, while those attached to the O-atoms (hydroxy groups, water) were located in residual electron-density maps. All were included in the refinement with isotropic U, using a riding model. For a summary of the crystallographic data for **5** see Table 1.

The experimental details related to compounds **6** and **7** have been documented elsewhere.[10] Those complexes also crystallized as nitrobenzene solvates with at least six molecules of nitrobenzene for each porphyrin framework contained in the crystal lattice.

Results and discussion

Bipyridyls **2**–**4** are excellent ligands for binding axially to, or bridging between, metalloporphyrins, as they can coordinate readily to the metal ion in the porphyrin core due to their high affinity for transition metals.[9] The pyridyl nitrogens, as well as the inner imino N-atoms (in **2** and **3**), are also very good proton acceptors for effective formation of hydrogen bonds with other components characterized by proton donating capacity (*e.g.* alcohols). On the other hand, porphyrin **1** may supramolecularly interact with the surrounding species by hydrogen bonding through the four hydroxy groups, exploiting its square planar functionality. Then, the OH polar functions are self-complementary, as each one of them may exhibit simultaneously proton donating and proton accepting behavior, thus allowing a direct self-assembly of **1** into extended arrays.[8] These features give rise to competitive modes of intermolecular aggregation. The length and type of the ligand, and possible presence of other polar species in the system (*e.g.* water) provide additional variants that may affect the preferential interaction scheme that forms.

Reaction of porphyrin **1** with ligand **2** yields a typical five-coordinate complex **5** in which the zinc ion adopts a square-pyramidal coordination environment, being displaced by *ca.* 0.29 Å from the porphyrin core towards the axial ligand [Fig. 1(a)]. The corresponding coordination distances are 2.012–2.022 Å to the inner pyrrole nitrogens and 2.155 Å to the pyridyl-N of the axial ligand. These complexes are held together by OH···OH hydrogen bonds (at O···O = 2.810 Å)

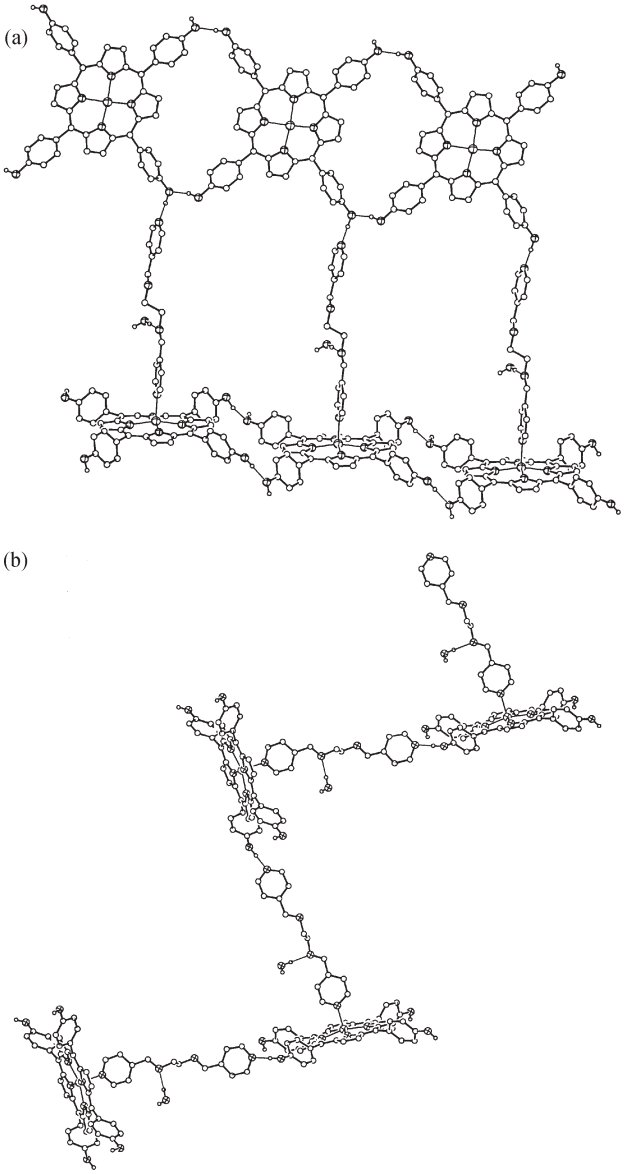

Fig. 1 Structure and supramolecular binding in complex **5** (**1**:**2**). (a) Linear porphyrin arrays sustained by cooperative hydrogen bonding between the *cis*-related arms of adjacent species displaced along the *a*-axis, which are also linked to each other by the bridging ligands. The latter simultaneously coordinate to the zinc ions of one array and hydrogen bond to the O–H···OH sites of another porphyrin array. (b) Side view of the terrace-like layer of interconnected species; projection down the *a*-axis of the crystal.

between the *cis*-related hydroxyphenyl arms on both sides of every unit, thus forming as the basic motif of this structure linear arrays of the porphyrin species that propagate parallel to the *a*-axis of the crystal. Every porphyrin unit is doubly linked, on both sides, to two adjacent moieties [Fig. 1(a)]. In the monoclinic space symmetry these arrays form a herring-bone arrangement with a nearly perpendicular orientation between hydrogen-bonded porphyrin chains related by the screw axis symmetry. In the resulting structure, the linear axial ligands sticking out of one array lie roughly in the plane, and hydrogen bond to the OH···OH sites of the perpendicular array. This yields corrugated (terrace-like) layers of the assembled species as shown in Fig. 1(b). A water molecule, hydrogen bonded to one of the inner nitrogens of the ligand (at OH···N = 2.902 Å; Fig. 1), provides two additional linkages between adjacent layers in the crystal by further interaction with the OH···OH binding sites (by proton donating to one OH group and proton accepting from another OH function). It bridges between layers

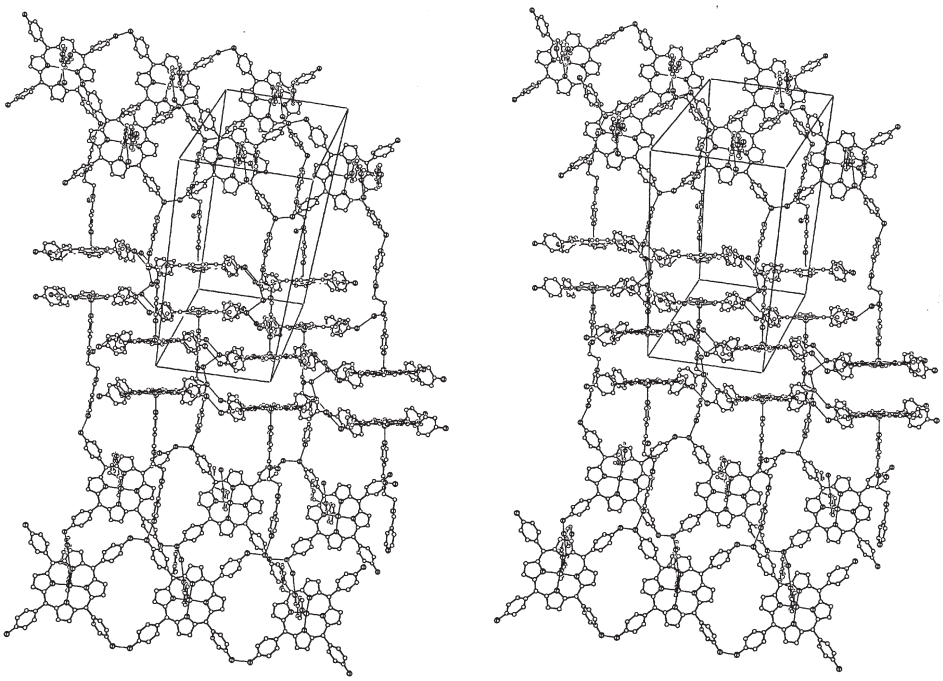

Fig. 2 Complex **5** (**1**:**2**): stereo view of the crystal structure (*a* is roughly horizontal and *c* is nearly vertical) which shows all types of the intermolecular non-covalent bonding observed in this lattice. Note the cross-linking of the inversion-related frameworks by the water molecule. Note also the 'back-to-back' arrangement of the porphyrin frameworks related by inversion. Click image or here to access a 3D representation.

displaced by unit translation along the *c*-axis of the crystal, as well as between those related by inversion (Fig. 2). The latter are arranged in a 'back-to-back' manner with the concave surfaces of the porphyrin rings facing one another. The van der Waals void space between these rings is 3–3.5 Å wide, adequate to accommodate a small aromatic moiety (such as nitrobenzene) edge-on.

The entire structure, shown in Fig. 2, thus represents a heterogeneous three-dimensional framework of extensively networked (by a combination of coordination and hydrogen bonding forces) molecules. All possible proton donors are utilized to capacity in these interactions. Open voids within the formed array, which make up *ca.* 43% of the crystal volume are accommodated by partly disordered nitrobenzene solvent.[14] Selected structural parameters related to the various synthons of the supramolecular interaction are summarized in Table 2.

The supramolecular motif described above differs to a considerable extent from that obtained by reaction of **1** with a somewhat shorter ligand **3** in essentially a non-aqueous environment (structure **6**).[10] In fact, the basic hair-comb-type structure in which the porphyrin units align in a hydrogen-bonded chain array and coordinate to the linear ligand in axial directions is preserved here as well. However, in this case, the top pyridyl group of every ligand coordinates perpendicularly to the metal ion core of another porphyrin moiety, creating a ladder architecture of thus assembled porphyrin and ligand components (Fig. 3). In order to satisfy the hydrogen bonding potential in this structure, additional ligand moieties are incorporated into the crystal lattice as good proton acceptors for the second OH proton of the inter-porphyrin OH···OH binding sites (Table 2). Every such ligand interconnects, by N···H–O hydrogen bonding on both sides, to diagonally displaced neighboring ladder assemblies, and creates extended networks (Fig. 4).

The large spacings between the porphyrin cores (*ca.* 16 Å) bridged by coordination within each ladder and by hydrogen bonding between adjacent ladders, along with the thermodynamic lability of the non-covalent interactions, give rise to the formation of an interweaved molecular organization. The ligand moieties, which connect sideways between two ladder assemblies, penetrate through the cavities between the hydrogen-bonded porphyrin units in a third ladder array (Fig. 3). The resulting supramolecular structure represents a porous, single-framework architecture sustained by a concerted mechanism of metal–ligand coordination and cooperative hydrogen bonding. The 6.5 Å wide cavities between the

Table 2 Selected structural parameters of coordination and hydrogen bonding in the supramolecular lattices of structures **5**–**7**

Complex	**5**	**6**	**7**[a]
Zn–N(pyrrole) bond length range/Å	2.063–2.082(2)	2.055–2.082(3)	2.021–2.063(5) 1.985–2.072(6)
Zn–N(axial pyridyl) distances/Å	2.168(2)	2.159(3)	2.134(6) 2.144(6)
Zn out-of-porphyrin-plane displacement[b]/Å	0.290(1)	0.313(2)	0.279(5) 0.280(5)
Inter-porphyrin OH···OH H-bonding distances/Å	2.688, 2.822	2.696, 2.810	2.637, 2.654, 2.702
Porphyrin–ligand OH···N H-bonding distances/Å	2.524	2.654, 2.648	—
Water–porphyrin O···O H-bonding distances/Å	2.668, 2.762	—	—
Water–ligand OH···N H-bonding distances/Å	2.902	—	—
O–H···X (X = O, N) hydrogen bond angle range/°	161–180	162–172	173–179

[a]There are two crystallographically independent porphyrin species, which reside on mirror planes, in the asymmetric unit of this structure. [b]Plane defined by the inner pyrrole N-atoms.

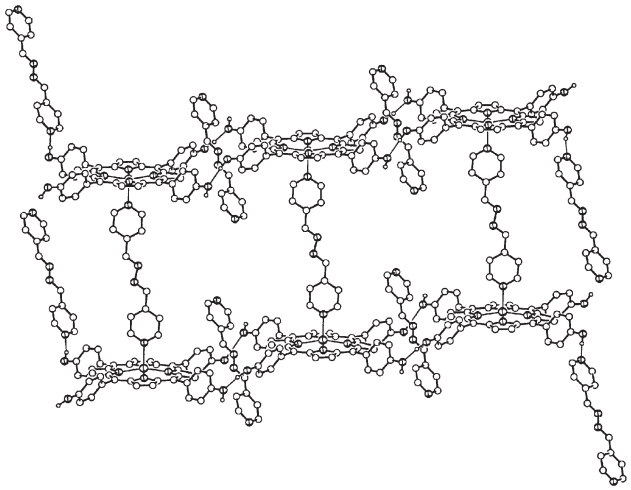

Fig. 3 Molecular recognition elements observed in complex **6** [(**1**)$_2$: (**3**)$_3$]. The porphyrin building blocks are interconnected by self-complementary hydrogen bonds. The resulting arrays are linked by bridging ligands that coordinate to the zinc centers of adjacent chains as shown. Other bipyridyl ligands (depicted on the left- and right-hand sides of the figure), directed sideways, provide additional hydrogen bonding bridges between porphyrin arrays displaced along other directions (see Fig. 4). It is also shown here that such bridges between two given arrays interpenetrate through the cavities of a third hydrogen-bonded porphyrin chain, thus yielding a concatenated structure.

molecular surfaces of the long thin ligands associated with this intermolecular organization (the solvent accessible space comprises 53% of the crystal volume)[14] are filled in the crystal by numerous non-coordinated molecules of the nitrobenzene solvent.

Another uniquely structured formulation of a three-dimensional supramolecular network was realized in **7**, formed by reaction of porphyrin **1** with ligand **4**. It represents a simultaneous expression of axial coordination and equatorial hydrogen bonding interaction potential of the porphyrin building block. The former involves ligand-mediated coordination between the porphyrin cores to form ligand-bridged porphyrin dimers [Fig. 5(a)]. The latter is represented by cooperative hydrogen bonding between the oligomeric units to yield a bi-layered open network with a square planar geometry, where every porphyrin moiety is linked by O–H···OH bonds to four different species [Fig. 5(a,b); Table 2].

The void space in these 2-D networks has a van der Waals width of *ca.* 15 Å, and is considerably larger than the size of a single porphyrin framework. On the other hand, the length of the bridging ligands is too short to allow their interpenetration through one porphyrin layer while still maintaining stable coordination to two other porphyrin layers (as in **6**). This gives rise to an interweaved organization of the porphyrin networks different than that in the previous example. In the present case, one bilayered array interpenetrates into the other by placing the porphyrin cores of one network in the center of the void space of another network. The concatenated bilayers are further interconnected to each other by additional hydrogen bonds, thus forming a three-dimensional, single-framework array of the porphyrin and ligand species [Fig. 6(a)]. The interporphyrin channels propagating perpendicular to the porphyrin bilayers [Fig. 6(a)] along with those running parallel to the porphyrin layers [Fig. 6(b)] make up the solvent-accessible void space in this lattice. These voids amount to *ca.* 62% of the crystal volume,[14] and are partly occupied in the analyzed crystals by diffused molecules of the nitrobenzene solvent.

The diversity of the porphyrin–ligand stoichiometry observed in these compounds deserves some further attention. One should keep in mind in this context that crystal formation is a cooperative process to obtain a stable (or sometimes metastable) condensed phase, while optimizing all intermolecular (specific and directional, as well as non-specific dispersive) interactions throughout the entire crystal. Structure **7** represents perhaps the most simple case in which the combined molecular recognition algorithm of cooperative coordination and hydrogen bonding, which plays an important role in the formation of supramolecular aggregates already in solution,[15] is expressed in the intermolecular organization. Thus, zinc-tetraarylporphyrins (due to the five-coordination preference of zinc) reveal high propensity for the formation square-pyramidal 1 : 1 complexes with pyridyl ligands or ligand-bridged 'porphyrin dimers' with bipyridyl species.[9] Next, in organic crystal structures all strong proton donors should be usually involved in hydrogen bonds with potential acceptor sites (Etter's hydrogen bond rules).[16] Then, metalloporphyrin solids reveal a largely conserved, corrugated layer pattern of parallel, offset-stacked porphyin components at typical intervals of *ca.* 4.5–5.0 Å.[17] The optimization of these three fundamental properties of the intermolecular interaction in the present system leads to a layered structure of 2 : 1 porphyrin–ligand oligomers (hence the 2 : 1 stoichiometry), hydrogen

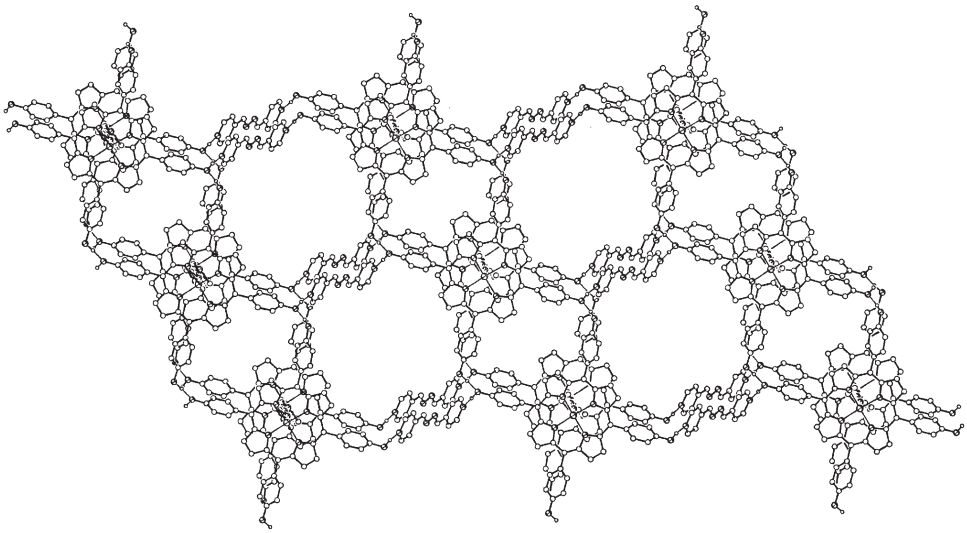

Fig. 4 Illustration of the heterogeneous supramolecular corrugated networks in **6** [(**1**)$_2$: (**3**)$_3$], projected on the porphyrin planes. These networks form by axial inter-coordination between the porphyrin cores by one ligand, and additional lateral hydrogen bonding between the ligand-bridged porphyrin dimers by other molecules of this ligand (**3**). Neighboring networks interpenetrate into one another by insertion of the hydrogen-bonded ligand through the cavity formed between the self-hydrogen-bonded porphyrin entities (see in Fig. 3).

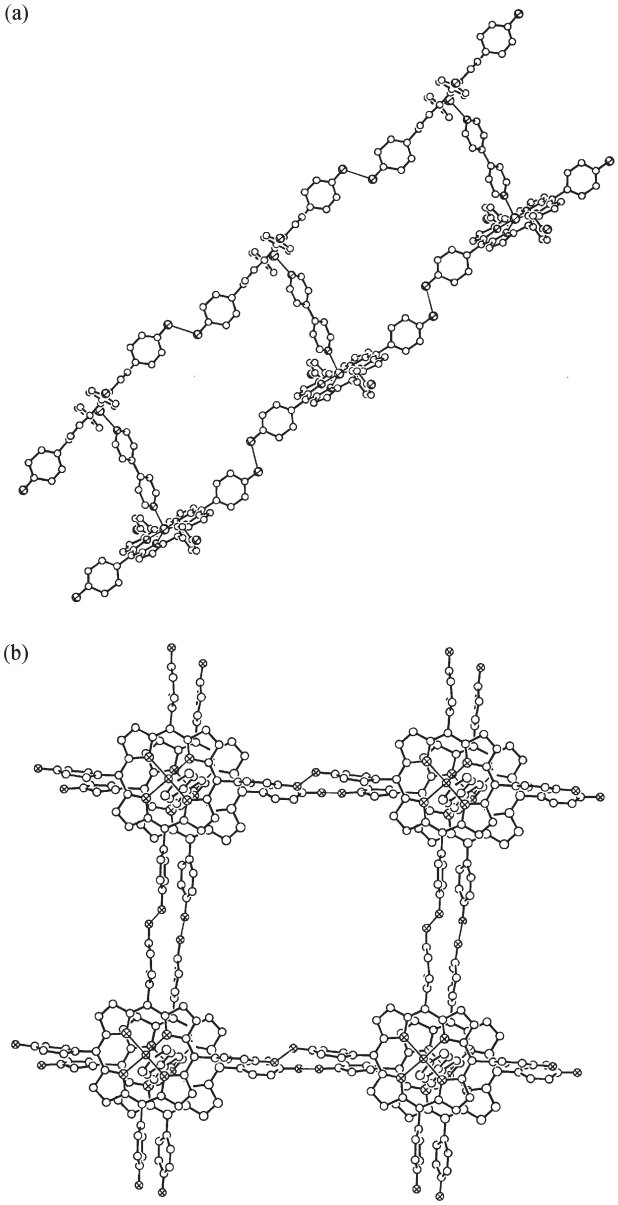

Fig. 5 Supramolecular assembly modes in complex **7** [(**1**)$_2$: **4**]. (a) Simultaneous coordination and hydrogen bonding (indicated by thin lines). The ligand auxiliary coordinates on opposite sides to the zinc centers of adjacent porphyrin cores. These ligand-bridged porphyrin dimers are further connected to each other sideways by inter-porphyrin O–H···OH hydrogen bonds, as shown in (b), yielding continuous, two-dimensional supramolecular arrays that extend throughout the crystal.

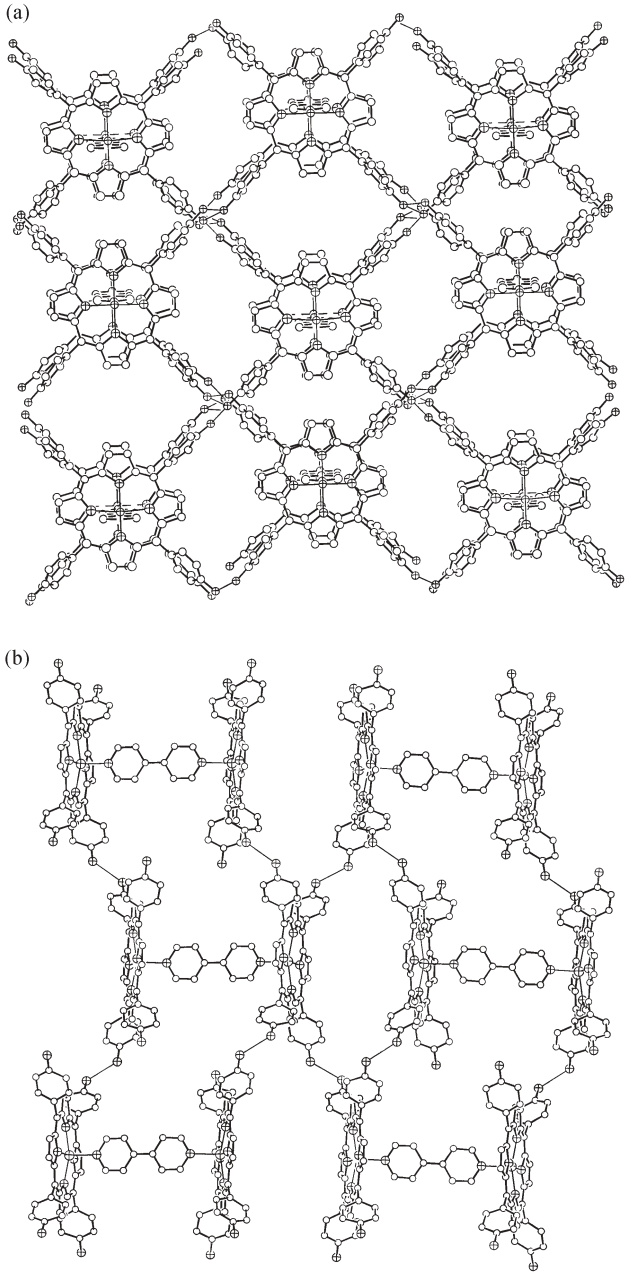

Fig. 6 Intermolecular organization in **7** [(**1**)$_2$: **4**]. (a) Interpenetrated assembly of parallel, hydrogen-bonded networks of the ligand-bridged dimers, projected approximately on the porphyrin plane. Note the multiple inter-porphyrin hydrogen bonding between adjacent porphyrin building blocks at every binding site. (b) Side view of the interlinked, ligand-bridged porphyrin dimers. A cross-section through four concatenated networks, showing the hydrogen bonding links between them.

bonded to each other in equatorial directions (Fig. 6). Ligand **4** fits almost perfectly here, holding the two porphyrin frameworks in the oligomeric cluster at a distance of approximately 9 Å, and allows the adjacent oligomer unit to interpenetrate in-between and hydrogen bond to one another. Formation of similar 'wheel-and-axle'-type 2 : 1 oligomers occurs with ligand **3** as well, except that in this case the longer ligand effects an inter-porphyrin spacing of *ca.* 16 Å. The latter does not allow a condensed, stack-layered arrangement of the porphyrin frameworks with simultaneous OH···OH hydrogen bonding in the two equatorial directions. Rather, the porphyrin–porphyrin hydrogen bonds extend along one direction (Fig. 3), while the two remaining 'unused' protons at every such O–H···OH site attract an additional ligand species (as a competitive proton acceptor) to utilize to capacity its binding potential.[16] This results in a 2 : 3 porphyrin : ligand ratio in structure **6**. The conformation of ligand **2** about its central, saturated C–C bond is usually *trans*, and it provides an inter-porphyrin spacer of *ca.* 14.3 Å when involved in the formation of a similar ligand-bridged 'porphyrin dimer'. This is associated with a considerable parallel offset of the two porphyrin 'wheels' due to the ligand conformation.[9a] The optimization of all possible OH···OH hydrogen bonds, while maintaining a layered organization of the porphyrin units, is not possible in this case either. The observed structure **5** represents, however, a less common herring-bone type of porphyrin crystal packing, in which the bridging ligand connects between two edge-to-face- rather than face-to-face-oriented chains of hydrogen-bonded porphyrins (Fig. 1). The characteristic porphyrin stacking arrangement[17] is limited in this structure to separated domains of the crystal (Fig. 2). In this pattern, which accounts for 1 : 1 porphyrin : ligand stoichiometry, all of the OH protons and the ligand

pyridyl sites are involved in intermolecular interactions, and there is no need to incorporate additional ligands. In view of the competing nature of the O–H···OH and O–H···N hydrogen bonds (even when identical preparative and crystallization conditions are applied), the preferential formation of the structural modes observed in **5** *vs.* **6** or **6** *vs.* **5** is not predictable.

Concluding remarks

The directional and relatively strong binding nature of metal–ligand coordination and multiple hydrogen bonding constitute effective synthons of intermolecular interaction, which leads to the formation of well organized, supramolecular, open lattices. Suitably functionalized porphyrin building blocks provide excellent tectons for the generation of stable two- and three-dimensional supramolecular architectures by concerted molecular recognition algorithms in the axial as well as equatorial directions, due to their rigidity, square shape functionality and ease of chemical modification. This has been confirmed in this study with the tetrahydroxyporphyrin tecton unit, as well as in previous successfully crystal-engineered structures based on the corresponding tetracarboxy and tetrapyridyl metallated-porphyrin derivatives.[7] Evidently, it is still not possible to reliably predict the type of supramolecular structure that may form in the crystal in a given case, due to the competitive nature of the weak, non-covalent interactions involved and because the crystal formation is severely affected by subtle differences in the crystallization environment (reflected often in pseudo-polymorphism). Yet, this and related studies indicate that homogeneous as well as heterogeneous porphyrin-based supramolecular lattices can be crystal-engineered effectively, including nano-porous structures resembling molecular-sieve materials, by a systematic utilization of self-complementary components and molecular recognition tools.[7] This provides a promising perspective for the design of new solid state receptors, heterogeneous catalysts and related molecular devices.

Acknowledgements

This research was supported in part by The Israel Science Foundation (Grant No. 68/01), as well as by the US–Israel Binational Science Foundation (BSF), Jerusalem, Israel (Grant No. 1999082).

Notes and references

1 J.-M. Lehn, *Supramolecular Chemistry – Concepts and Perspectives*, VCH, Weinheim, 1995.
2 J. K. M. Sanders, N. Bampos, Z. Clyde-Watson, S. L. Darling, J. C. Hawley, H.-J. Kim, C. C. Mak and S. J. Webb, in *The Porphyrin Handbook*, K. M. Kadish, K. M. Smith and R. Guilard, ed., Academic Press, London, 2000, **vol. 3**, ch. 15, pp. 1–48; J.-C. Chambron, V. Heitz and J.-P. Sauvage, in *The Porphyrin Handbook*, K. M. Kadish, K. M. Smith and R. Guilard, ed., Academic Press, Orlando, FL, 2000, **vol. 6**, ch. 40, pp. 1–42.
3 G. R. Desiraju, *Angew. Chem., Int. Ed. Engl.*, 1995, **34**, 2311; F. Allen, P. R. Raithby, G. P. Shields and R. Taylor, *Chem. Commun.*, 1998, 1043.
4 For example: V. S.-Y. Lin, S. G. DiMagno and M. J. Therien, *Science*, 1994, **264**, 1105; S. Prathapan, T. E. Johnson and J. S. Lindsey, *J. Am. Chem. Soc.*, 1993, **115**, 7519.
5 Y. Diskin-Posner and I. Goldberg, *Chem. Commun.*, 1999, 1961.
6 Y. Diskin-Posner, S. Dahal and I. Goldberg, *Angew. Chem., Int. Ed.*, 2000, **39**, 1288.
7 I. Goldberg, *Chem. Eur. J.*, 2000, **6**, 3863; I. Goldberg, *CrystEngComm*, 2002, **4**(20), 109.
8 I. Goldberg, H. Krupitsky, Z. Stein, Y. Hsiou and C. E. Strouse, *Supramol. Chem.*, 1995, **4**, 203.
9 (*a*) Y. Diskin-Posner, G. K. Patra and I. Goldberg, *J. Chem. Soc., Dalton Trans.*, 2001, 2775; (*b*) R. Krishna Kumar, Y. Diskin-Posner and I. Goldberg, *J. Inclusion Phenom.*, 2000, **37**, 219.
10 Y. Diskin-Posner, G. K. Patra and I. Goldberg, *Chem. Commun.*, 2002, 1420.
11 Nitrobenzene turned out to be an excellent template for the stabilization of open multiporphyrin assemblies. See examples in ref. 5, as well as in B. F. Abrahams, B. F. Hoskins and D. M. Michail, *Nature*, 1994, **369**, 727.
12 P. T. Beurskens, G Admiraal, G. Beurskens, W. P. Bosman, S. Garcia-Granda, R. O. Gould, J. M. M. Smits and C. Smykalla, The DIRDIF-96 Program System, Technical Report of the Crystallography Laboratory, University of Nijmegen, The Netherlands, 1996.
13 G. M. Sheldrick, SHELXL-97: Program for the Refinement of Crystal Structures from Diffraction Data, University of Göttingen, Germany, 1997.
14 The solvent-accessible volume was assessed in these structures using the PLATON software: P. Van der Sluis and A. L. Spek, *Acta Crystallogr., Sect. A*, 1990, **46**, 194; A. L. Spek, *Acta Crystallogr., Sect. A*, 1990, **46**, C34.
15 E. B. Fleischer and A. M. Shachter, *Inorg. Chem.*, 1991, **30**, 3763; X. Shi, K. M. Barkigia, J. Fajer and C. M. Drain, *J. Org. Chem.*, 2002, **66**, 6513.
16 M. C. Etter, *J. Phys. Chem.*, 1991, **95**, 4601.
17 R. Krishna Kumar, S. Balasubramanian and I. Goldberg, *J. Inorg. Chem.*, 1998, **37**, 541; M. P. Byrn, C. J. Curtis, Y. Hsiou, S. I. Khan, P. A. Sawin, S. K. Tendick, A. Terzis and C. E. Strouse, *J. Am. Chem. Soc.*, 1993, **115**, 9480.